2023-08

Black-odorous water bodies annual dynamics in the context of climate change adaptation in Guangzhou City, China

Liu, B

10.1016/j.jclepro.2023.137781
Journal of Cleaner Production
Elsevier BV

Black-odorous water bodies annual dynamics in the context of climate change adaptation in Guangzhou City, China

Abstract: Black-odorous water (BOW) in urban areas has brought detrimental ecological effects and posed a threat to the health of surrounding residents. Identifying BOWs in urban areas is difficult because they are usually small in area, and discontinuous in spatial distribution. The efforts to adapt to climate change in cities have a direct connection to urban environment and may affect the dynamics of BOWs, but their relationship has seldom been addressed in previous research. This research builds a new urban BOW detection model using Gaofen (GF) images and ground-level in-situ water quality data to detect the spatiotemporal dynamics of BOWs in Guangzhou City's main urban area from 2016 to 2020, when comprehensive climate adaptation strategy has been implemented as a pilot metropolitan area in China. Spatial analysis in the study area with a total of 97 focused rivers revealed a decreasing trend in BOW occurrence (from 85.57% in 2016 to 21.65% in 2020) in the context of climate change adaptation efforts. Redundancy analysis between BOWs occurrence and environmental factors showed that across the entire study area, the contributions of anthropogenic factors (highest proportion at 14.3% for the area percentage of built-ups) to BOW, such as population density, agricultural water use, domestic water use, and so on, distinctly stronger than climatic drivers (largest contribution of 4.4% for temperature). The results suggested that climate change adaptation efforts help to decrease BOW occurrence in the study area, while exploring the response mechanism between climate change adaptation measures and the changes of BOWs be necessary in the future research. The findings were conducive to the development of targeted measures to decrease the occurrence of urban BOWs while improving adaptability of the city to climate change.

Keywords: black-odorous water, detection model, GF images, climate change adaptation, spatiotemporal trends, Guangzhou

1. Introduction

Black-odorous water (BOW) is a typical urban water environment problem, and it has brought detrimental ecological effects and posed a threat to the health of surrounding residents. Urban BOW occurs worldwide both in developed and developing countries (Wang et al., 2019a), such as the United States(Barnes et al., 2014), Australia (Hladyz et al., 2011), India(Rixen et al., 2010) and China(He et al., 2018). As the water environment suffers from organic pollution that exceeds its self-purification capacity, the aerobic decomposition of organic matter causes oxygen deprivation(Cao et al., 2020), generating odoriferous and black substances(Li et al., 2020a; Norgbey et al., 2021).

Global climate change is one of the most significant challenges facing humanity, leading to temperature increase and extreme weather events (Hersbach et al., 2020; Sonali and Kumar, 2020). Given the complex structure, high population density, and intense human activities, cities were particularly affected by climate change(Estrada et al., 2017). Accordingly, some large cities had incorporated climate change into their long-term development strategies and made efforts to improve their adaptivity to climate change (Malhi et al., 2020). There is a growing recognition that water is central to climate change adaptation. Among the contributions identified by 79% of countries, water is a top adaptation priority(Robiou du Pont et al., 2017).

Climate change increases the complexity and uncertainty of the formation of BOW, because changes in precipitation and temperature can affect water quality by altering dilution and transport processes and by affecting the degradation of river pollutants(Bartlett and Dedekorkut-Howes, 2022; Santy et al., 2020). On the other hand, climate change adaptation measures such as improving and rehabilitating urban drainage networks, improving the capacity to optimize water allocation, and enhancing urban ecological restoration (Babaeian et al., 2021; Biswas et al., 2022) have been individually proven to have an impact on the occurrence and severity of BOWs. Poor water resource management exacerbated the impact of climate change on BOW(Cherkauer et al., 2021). BOW bodies were also closely related to urban drainage systems when precipitation occurs(Xu et al., 2019b). In China, urban stormwater drainage systems may not be able to withstand sudden rainfall events, resulting in low wastewater collection rates(Xu and Xu, 2022). Moreover, the separation of stormwater and wastewater drainage systems may lead to contamination of water bodies by initial rainfall(Liao et al., 2016; Xu et al., 2021c), which improved the complexity of spatiotemporal changes of BOWs. In addition, anthropogenic and natural factors increased risks of the rebound in BOW presence in urban areas(Wang et al., 2022). So far, climate change adaptation in urban areas currently focuses on the planning and implementation of actions. There are limited studies to assess whether multifaceted climate change adaptation measures have been successful in reducing the BOW spatiotemporal dynamics in urban areas (Berrang-Ford et al., 2021).

Accurately identifying BOW distribution is prerequisite to analyze the impacts of climate change adaptation to BOW dynamics. Identifying BOWs in urban areas is difficult because they are usually small in area, and discontinuous in spatial distribution. For small urban rivers, images with less than 5 m spatial resolution are generally needed to monitor their water quality(Wen et al., 2018). The development of high spatial resolution satellite data, such as the GF2 satellite, facilitated time-series analysis aiming at spatiotemporal trends(Fang et al., 2022) of BOW. There are unique spectral characteristics of BOW that distinguish it from normal water bodies(Miao et al., 2021; Yu et al., 2022). Many studies adopted spectral band combinations as input and classified the BOW model results into different levels by selecting thresholds for empirical models of BOW identification(Li et al., 2019a; Qi et al., 2020). The Commission Internationale de L'Eclairage(CIE) method(Shen et al., 2019) or the nutrient status index based on chlorophyll-a(Chla) or total suspended solids(TSS) were also constructed to identify BOWs. In addition, machine learning methods have been applied to BOW identification(Sarigai et al., 2020; Zhou et al., 2022) but are limited because of inadequate samples. The accuracy of the model to identify the distribution of BOW over the years and the possibility of differences in the dominant factors of regions with different characteristics need to be taken into consideration. In recent years, with the enhancement of BOW management, there have been obvious changes of BOW bodies in many cities(Cao et al., 2020), while most BOW models lack applicability to different types of regional and interannual variability(Yu et al., 2022).

Due to its advantages of periodicity and repeatability, remote sensing data has proved to be cost-effective in monitoring water environment changes, and current studies were mainly carried out in inland lakes(Hu et al., 2022) and coastal areas(Zhu et al., 2022), among which the mostly investigated parameters include Chla(Cao et al., 2022; Chen et al., 2022) or algal bloom(Fang et al., 2022), TSS (Du et al., 2022a), Secchi Disk depth(SD) or transparency (Somasundaram et al., 2021; Song et al., 2022; Zhao et al., 2021), etc. However, there have been few studies on the spatial-temporal changes of small BOW bodies in urban areas (Zhou et al., 2022), especially in the context of climate change adaptation.

With Guangzhou, China, selected as the study area, where a range of climate change adaptation measures has been implemented, the present study aims: 1) to develop an efficient and convenient BOW detection model for urban areas with high-resolution remote sensing images; 2) to explore annual spatial-temporal variations of BOWs from 2016 to 2020 in the context of climate change adaptation; and 3) to quantify the contribution of climate change and human activities related to climate change adaptation upon BOW bodies annual dynamics. The results will provide valuable insights for implementing climate change adaptation while eliminating BOWs in urban areas.

The rest of the paper is structured as follows: Section 2 describes the study area and its climate change adaptation measures, research framework, satellite image processing, the new BOW model, BOW driver selection, and analysis methods. Model validation of the BOW model, spatiotemporal variations of BOWs from 2016-2020, contributions of climate change and anthropogenic drivers are presented in Section 3. Section 4 examines the applicability of the BIR model, BOWs variation in the context of climate change adaption, limitations of the present study, and policy implications. Finally, the conclusion was provided in Section 5.

2. Data and Methods

2.1. Study area and its climate change adaptation measures

Guangzhou, the capital city of Guangdong Province, is a highly developed urban center(Yi et al., 2019) characterized by a dense river network and a plain landscape. This study focuses on the main urban area of Guangzhou, China (Fig. 1) which was obtained based on the global impervious surface data (GAIA) (Li et al., 2020b). The total area of the study area covers 1,110 km^2. A large number of rivers in Haizhu District are sensitive to tides and dissolved oxygen (DO) content fluctuates day and night. Despite the rapid economic growth, the study area faces severe water pollution issues due to the increasing amount of sewage discharge and relatively inadequate urban environmental infrastructure, and uncertainty of precipitation caused by climate change (Xu et al., 2019a). In 2015, 138 BOW bodies were included in the key regulatory list of Guangzhou(Cao et al., 2020), the largest number among cities in China, and later expanded to 197 in 2018. Although these BOW bodies were declared to have been eliminated in 2020, some areas still suffer from the rebound phenomenon of

BOW for the lack of source control treatment(Ministry of Housing and Urban-Rural Development of the People’s Republic of China, 2021).

Guangdong Province's climate has undergone significant changes in the context of global warming. Since 1961, the average temperature in the province has increased by 0.19°C per decade, which is higher than the global average (0.15°C per decade) (People's Government of Guangdong Province, 2011). Annual precipitation and total water resources show a small cycle of abundance and deficit around the normal level in the province; however, the variability of precipitation has increased, leading to more extreme precipitation events (Wai et al., 2017).

In 2017, Guangdong Province issued the "Guangdong 13th Five-Year Plan for Climate Change Adaptation" proposing a series of measures to enhance the province's ability to adapt to climate change. Among them, the ecological environment measures play a significant role in influencing BOW. To optimize and rationalize the use of water resources, replacing old urban water supply pipelines and promoting the utilization of rainwater were adopted. For strengthening water pollution control and water ecological protection, the plan proposes strengthening the treatment of urban domestic sewage, improving sewage pipelines and treatment facilities, controlling agricultural non-point source pollution, and purifying agricultural drainage and surface runoff (Development and Reform Commission of Guangdong Province, 2017). And now Guangdong Province is developing a comprehensive climate adaptation strategy addressing both urban planning and industrial structural readjustment to reduce the reliance on fossil fuel consumption in economic development, while improving regional resilience to water-related disasters. Measures such as optimizing water management, promoting sponge cities, and improving the efficiency of wastewater treatment plants were proposed in the city's 14th five-year plan (Development and Reform Commission of Guangdong Province, 2022).

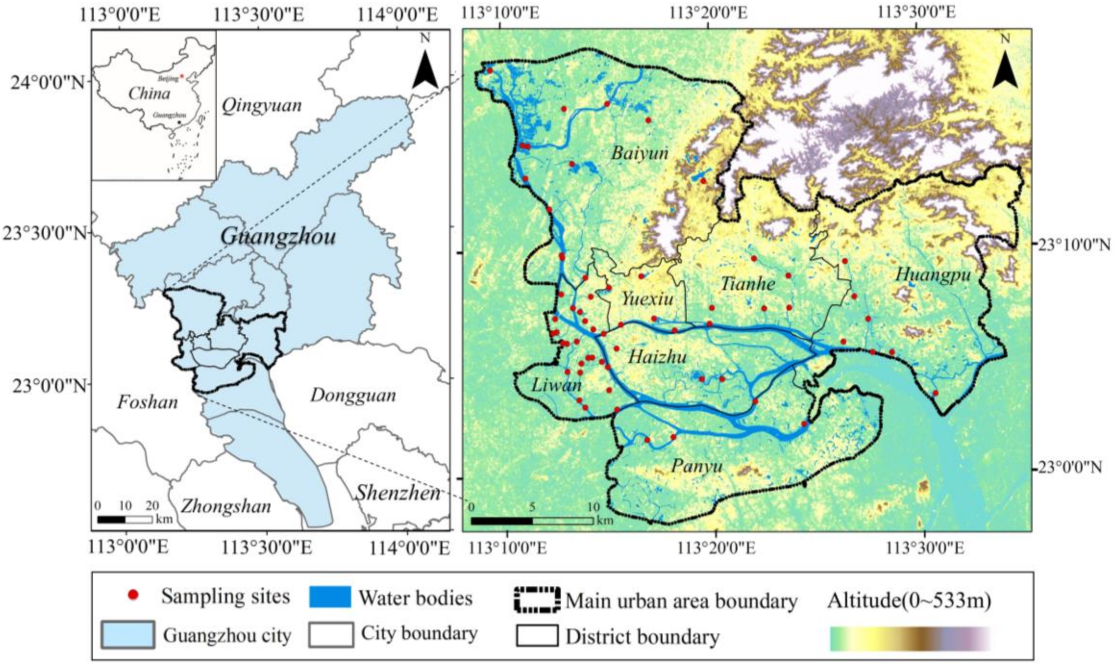

Fig. 1 The study area of Guangzhou City.

2.2. Research framework

The research framework is illustrated in Fig. 2. A new BOW model was established in section 2.5 and validated in section 3.1. Spatial distribution and temporal variations of BOW from 2016 to 2020 were shown and counted in section 3.2. The effects of climate change and human activities on BOW were displayed by analyzing the correlation and contributions of BOW drivers with the redundancy analysis (RDA) method in sections 3.3 and 3.4. Further interpretation of BOW variations and policy implications with climate change adaptation were discussed in section 4.

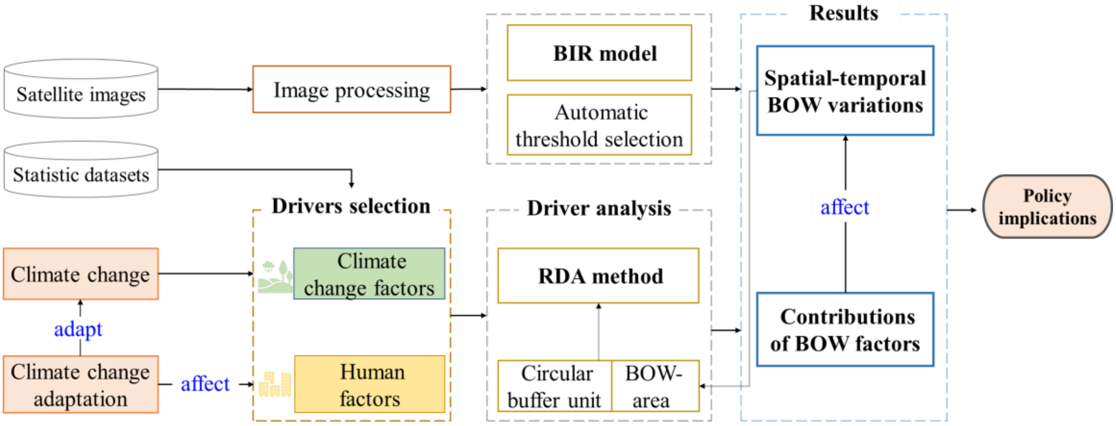

Fig. 2 Research framework.

2.3. In-situ water quality data

Water quality data of key rivers in Guangzhou were collected in two ways: 1) automatic monitoring stations; 2) historical water quality data obtained by manual sampling monthly from 2016 to 2020, published by the *Guangzhou Municipal Ecological Environment Bureau* (http://112.94.69.56:8022/index.html#/gzhbapp-riverWaterQuality-pc). The data contain three indicators, namely ammonia nitrogen (NH_3N), DO, and SD (only for 2016). The data were collected from 36, 56, 60, 61, and 62 sampling points from 2016 to 2020, respectively, and some data were missing in some years. Specially, the time gap between the data collected from the automatic monitoring stations and the satellite image transit was 0.5 h. The study adopted the single indicator method from the BOW standard (Ministry of Housing and Urban-Rural Development of the People's Republic of China, 2015), i.e. if one indicator exceeds the specified value, the sample is determined as a BOW(Miao et al., 2021). In the practical management in Guangzhou, NH_3N is used as the primary criterion for BOW determination. In this study, NH_3N and DO were used to classify BOW levels. If NH_3N and DO of a sample exceed the standard values, it is sufficient to identify the sample as BOW.

2.4. Satellite images and processing

2.4.1. GF imagery selection

20 scenes of GF-1 and GF-2 images from 2016 to 2020 were collected, and their details are provided in Table 1.

Table 1. Satellite images used in this paper

Type	Imaging Time	Scenes	Spatial Resolution for GF images		
GF-1	2016-12-07	4	GF-1 PMS	Panchromatic	2m
GF-2	2017-09-15	6		Multispectral	8m
GF-1B	2018-10-07	2	GF-1 B/D	Panchromatic	2m
GF-1D	2018-09-11	1		Multispectral	< 8m
GF-1	2019-09-28	2	GF-2 PMS	Panchromatic	0.8m
GF-2	2020-11-26	5		Multispectral	3.2m

China's GF-1 and GF-2 are high-resolution Earth observation satellites launched in 2013 and 2014, respectively. They capture images with high-spatial resolution and have multiple bands including 1 panchromatic and 4 multispectral (Blue, Green, Red and Near-infrared) bands. GF images are currently suitable for urban water quality studies because of their sub-meter level of spatial resolution accuracy.

2.4.2. Image preprocessing

Five steps were applied before water extraction. First, the geometric correction was performed. Second, these images were radiometrically calibrated and atmospherically corrected using the FLAASH model in *ENVI 5.3* software. Then the Gram-Schmidt Pan Sharpening method was utilized to fuse the panchromatic and multispectral bands to obtain higher spatial resolutions, and the infused spatial resolutions of GF-1 and GF-2 images were 2 m and 1 m respectively. Four, the image mosaic is necessary to provide image information for an entire study area. Finally, mosaiced images were clipped using boundary shape files of the study area to facilitate water surface extraction and the BOW model calculation.

Water extraction is an essential part. Shadows from the densely packed tall buildings and asphalt streets in Guangzhou contaminated the images, making it difficult to extract small water bodies from images (Bie et al., 2020). To attenuate the interference of roads and shadows on water body classification, the four bands of the GF images were combined with the normalized difference water index (NDWI), and then classified with maximum likelihood classifier. The overall accuracies and kappa coefficients of water body extraction were all above 87% and 0.87 (shown in Table S1), adequate for water quality parameters retrievals(Zhao et al., 2021). To ensure the reliability, water bodies less than 50m^2 were not used in further analysis.

2.5. BOW model and optimal thresholds

A total of 88 image samples at corresponding in-situ sites were selected to construct a new BOW model, including 46 ordinary water samples and 42 BOW samples on September 15, 2017. Additionally, 18 in-situ water quality samples were selected based on automatic water quality monitoring stations. 51 image sampling points were located close to an automatic monitoring station, the bend of a river, in slow-flow zones, and near residential areas, for the water quality at these points was nearly equivalent to that of the nearest automatic monitoring station.

2.5.1. BOW identification model

The image reflectance of BOW and ordinary water differs across several GF bands (Fig. S1). Aiming at amplifying the difference between BOW and ordinary water, the present study constructed an index, namely BOW by Image Reflectance (BIR), as shown in Eq. (1).

$$BIR = \frac{(\text{NIR-R})/(\lambda_{\text{NIR}}-\lambda_{\text{R}})}{(\text{G-R})/(\lambda_{\text{R}}-\lambda_{\text{G}})} = \begin{cases} \leq threshold, & Ordinary\ water \\ > threshold, & BOW \end{cases} \tag{1}$$

where, B, G, R, and NIR represent remote sensing reflectance in the blue, green, red, and near-infrared bands respectively. λ_{G}, λ_{R}, λ_{NIR} are central wavelengths of the green, red, and near-infrared bands. For GF-2, $\lambda_{\text{G}} = 555$ nm, $\lambda_{\text{R}} = 665$ nm, and $\lambda_{\text{NIR}} = 821$ nm. For GF-1, $\lambda_{\text{G}} = 576$ nm, $\lambda_{\text{R}} = 680$ nm, and $\lambda_{\text{NIR}} = 810\ nm$.

2.5.2. Optimal BOW threshold with automatic discrimination algorithm

57 training samples were randomly selected from the total 88 samples and comprised 29 ordinary water samples and 28 BOW samples. The remaining 31 samples were testing samples, consisting of 17 ordinary water samples and 14 BOW samples. Using the training samples, the recognition accuracy $T\_accuracy_i$ and the optimal threshold T_{best} were calculated by Eq. (2).

$$T_{best} = Max(T\_accuracy_i) = Max(\frac{(\sum CN_{train})_i}{N_{train}}) \tag{2}$$

where i = 1, … 57 refers to the *i*-th training sample; $\sum CN_{train}$ is the sum number of correctly recognized BOW and ordinary samples for a given threshold, and N_{train} = 57. The best threshold corresponds to the BIR model value which achieves the highest value of $T\_accuracy_i$.

To enhance the recognition accuracy of BOW, it is necessary to calibrate the threshold value for each year of the BIR model. This can be achieved by applying the Automatic Threshold Selection of BOW (ATSB) algorithm in Eq.(2) using *Matlab 2021a*. Additionally, statistical characteristics and the Mann-Whitney U nonparametric test were used to determine if training and testing samples were randomly distributed(Cardew, 2003) with *IBM SPSS Statistic 20*.

2.5.3. Model accuracy assessment

To assess the accuracy of BOW models, overall recognition accuracy (RA) (Eq.3) and kappa coefficient (Eq.4-6) were calculated with test samples.

$$RA = \frac{CN_{test}}{N_{test}} \times 100\% \tag{3}$$

where CN_{test} is the number of testing samples correctly recognized, including ordinary water (ORW) and BOW samples, and N_{test} is the total number of testing samples.

$$Kappa = \frac{RA - Pe}{1 - Pe} \tag{4}$$

$$Pe = \frac{CN_{ORW} \times N_{ORW} + CN_{BOW} \times N_{BOW}}{N_{test}^2} \tag{5}$$

$$RA_{ORW} = \frac{CN_{ORW}}{N_{OR}} \times 100\% \tag{6}$$

$$RA_{BOW} = \frac{CN_{BOW}}{N_{BOW}} \times 100\% \tag{7}$$

Where RA_{OR} and RA_{BOW} are recognition accuracies of ordinary water and BOW respectively. CN_{OR}, and CN_{BOW} are the numbers of correctly recognized ordinary water and BOW respectively, and N_{OR} and N_{BOW} are amounts of the test samples for ordinary water and BOW in the same order.

2.6. BOW drivers affected by climate change adaptation

To explore how environmental factors make changes in BOW bodies, potential BOW drivers that would be influenced by climate change and its adaptation and directly contribute to the formation and development of BOW should be selected in preference. Natural impacts are mainly from climate change(Xu et al., 2021b) and are normally represented by Temperature and Precipitation. Anthropogenic factors correspond to human activities and reflect the results of climate change efforts made in Guangzhou. These factors include two parts, namely urban expansion, water use and discharge. Urban expansion is often reflected in terms of built-up area and population density. Land use and land cover change(LUCC), especially in urban and industrial areas(Song et al., 2022), are the main drivers of water quality degradation(Bhat et al., 2021; Zhao et al., 2015). The impervious surface area has a significant effect on total phosphorus (TP), total nitrogen (TN), and DO(Li et al., 2019b; Wang et al., 2021). It is essential to analyze the impact of LUCC on water quality in high-speed urbanized areas(Lin et al., 2021; Liu et al., 2022). Population density is often used as a driving factor in water quality for its direct correlation with human activities(Bhat et al., 2021). Water use and discharge include water consumption and discharge. Insufficiently regulated discharge of wastewater is the primary contributor to water pollution(Jones et al., 2022). Industrial wastewater, domestic sewage, and fertilizer from human life and industrial process(Lin et al., 2021), flow into urban rivers and lakes through point and surface sources of pollution, leading to eutrophication and even blackening water bodies(Ren et al., 2018; Song et al., 2021).

Data for potential natural and anthropogenic factors from 2016 to 2020 were collected (Table 2). Population data was validated with satisfying accuracy by *Guangzhou Statistical Yearbook*. Built-ups represent the percentage of built-up area to the total area of a region, revealing the intensity of exposure to human activities(Zhao et al., 2022). Besides, the area percentage of BOW bodies to the total water surface (extracted from 2.4.3), called the BOW-area, can quantify the effect of these factors on BOW changes. Therefore, the BOW-area was adopted as a dependent variable, and the value of each factor was regarded as another independent variable to analyze their relationships.

Table 2. The data source for the BOW factors

Factor types	**Data**[a)]	**Unit**	**Resolution**		**Source**	**Url**
			Temporal	**Spatial**		
Climatic change	Pre	0.1mm	monthly	1km	the National Earth System Science Data Center	http://www.geodata.cn
	Tmp	0.1°C	monthly	1km		
Urban expansion	Pop	person/km^2	annual	1km	LandScan	https://landscan.ornl.gov/
	Built-up area	pixel	annual	1m/2m	LUCC from section 2.4.3 in this paper	-
Water use and discharge	Wastewater	t/person	annual	- [b)]	Guangzhou Water Resources Bulletin	http://slt.gd.gov.cn/szygb/
	Agricultural water	m^3/person	annual	-		
	Industrial water	m^3/person	annual	-		
	Domestic water	m^3/person	annual	-		

[a)] Pre = precipitation; Tmp = temperature; Pop = population density; Wastewater = wastewater discharge; Agricultural water = agricultural water use; Industrial water = industrial water use; Domestic water = domestic water use; Built-up area = the area of built-ups.

[b)] Not applicable.

BOW-area and Built-ups here are calculated with buffer zones as the calculation units. Bhat et al. (2021) found that the reach-scale (500 m wide section) explained slightly better (76%) variations in water quality than riparian (75%) and watershed (70%) scales. In areas with high anthropogenic impacts, such as rapidly urbanizing areas, circular buffers are crucial for conservation efforts(Song et al., 2020). Human activities and the presence of artificial river systems and ponds in Guangzhou make BOW bodies highly susceptible to changes. Consequently, using watersheds, normally retrieved by digital elevation model, as analysis units are impracticable. Instead, LUCC within buffers can have a more direct and effective impact on water bodies(Liu et al., 2021). Using *ArcGIS 10.4* software, the hydrological unit boundary was established by forming a circular buffer zone with a radius of 200m around the water quality monitoring station as the geographic center.

2.7. Data analysis methods

Here, spearman correlation analysis in Eq.(8) was adopted to determine the relationship r between BOW-area and each environmental factor variable, both in the direction (positive or negative) and strength (2-tailed significance test)(Du et al., 2022b). The correlations between the BIR model and water quality parameters were also analyzed with the same method.

$$r = \rho_{R(X),R(Y)} = \frac{\mathrm{cov}(\mathrm{R(X)}, \mathrm{R(Y)})}{\sigma_{R(X)}\ \sigma_{R(\mathrm{Y})}} \tag{8}$$

where, ρ denotes the usual Pearson correlation coefficient, but applied to the rank variables, $\mathrm{cov}(\mathrm{R(X)}, \mathrm{R(Y)})$ is the covariance of the rank variables, $\sigma_{R(X)}$ and $\sigma_{R(\mathrm{Y})}$ are the standard deviations of the rank variables.

To better explicate the influence of environmental drivers on BOW changes, RDA was conducted to calculate the relative contribution(Wang et al., 2019b) to explore how the environment affected the conditions of BOW bodies. The greatest advantage of RDA is that the contribution of each factor to the BOW-area can be maintained independently, effectively providing a statistical test for multiple explanatory variables(Cheng et al., 2018). RDA can be understood as a two-step process(Legendre and Legendre, 2012) in Eq.(9)-(10). ${R^2}_{Y|X}$ measures the strength of the canonical relationship between Y and X by Eq. (11); Adjusted R^2 (${R^2}_a$) in Eq. (13) applies a correction of the R^2 to take into account the number of explanatory variables.

$$Y_{fit} = X[X'X]^{-1}X'Y \tag{9}$$

$$Z_{fit} = Y_{fit}U \tag{10}$$

$$R^2{}_{Y|X} = \frac{SS(Y_{fit})}{SS(Y)}) \tag{11}$$

$$Z_{res} = (Y - Y_{fit})U_{res} \tag{12}$$

$$R^2{}_a = (1 - (1 - R^2{}_{Y|X})\frac{(n-1)}{(n-m-1)}) \tag{13}$$

where, X is an explanatory matrix for explanatory variables, and Y is a response matrix. The first step in Eq. (9) regresses each variable in Y on all variables in X and computes the fitted values Y_{fit}. Then the second step in Eq. (10) carries out a PCA of the matrix of fitted values to obtain the matrix of eigenvectors, namely U and U_{res}. The space of explanatory variables X is obtained as Z_{fit}. In Eq. (11), $SS(Y_{fit})$ is the total sum of squares of Y_{fit}, and $SS(Y)$ is the total sum of squares of Y. Another PCA ordination, Z_{res}, can be computed in Eq. (12) for the matrix of residuals. In Eq. (13), m is the number of explanatory variables in X.

Combining the characteristics of administrative districts and watersheds, the study area was divided into four sub-regions to calculate the contributions of drivers. Liwan District (L) and Baiyun District (B) were respectively separate sub-regions; Yuexiu, Tianhe, and Huangpu districts were combined into one group named YTH, as a sub-region; and Haizhu and Panyu districts were formed as a group named HaP. Standardized data of factors were input into *Canoco for Windows 4.5 RDA* software and the significance of the variables was tested by the Monte Carlo method.

3. Results

3.1. Validation of the BOW identification model

The optimal threshold selection (Fig. S2), overall accuracy, and kappa coefficients were obtained from the best-performing combinations of bands for the BIR model. It achieved the best overall recognition accuracy of 96.8%, with a BOW recognition accuracy of 92.9%, ORW accuracy of 100%, and a kappa coefficient of 0.98. Meanwhile, Mann-Whitney U nonparametric test showed no significant differences between training and testing samples (Table S2). There are significant differences in three BOW determination indicators (NH_3N, DO, and SD) and BIR values between ORW and BOW bodies (Fig. S3), illustrating a good performance of the BIR model in separating BOWs and ORWs.

The detection accuracies of BIR with the optimal thresholds for the years 2016-2020 were also calculated (Table 3). The overall accuracy was greatly improved after the threshold adjustment, such as the RA in 2016 from 66.67% to 91.67%. Especially, even for the images in 2017, the threshold correction was still required to apply to the main urban area. Meanwhile, there is an increasing trend of optimal thresholds over the past years.

Table 3. Threshold correction results and recognition accuracy

Year	Before adjustment		After adjustment	
	Original threshold	Corresponding RA	Adjusted threshold	Corresponding RA
2016	0.62	66.67%	0.26	91.67%
2017	0.62	82.14%	0.54	87.50%
2018	0.62	73.21%	2.94	90%
2019	0.62	59.02%	2.08	90%
2020	0.62	90.32%	- [a]	-

[a] “-” represents “not adjusted”, because there is no BOW sample for that year and the threshold correction to Eq. (1) cannot be performed. Therefore, the threshold for the BOW recognition model in 2020 is kept at 0.622 without adjustment.

3.2. Spatiotemporal variations of BOWs

With the adjusted thresholds for the BIR model, the spatial distributions of BOW bodies in the main urban area of Guangzhou City from 2016 to 2020 were obtained and shown in Fig. S4. BOW bodies showed a significant decreasing trend in the entire study area, despite obvious variations in different regions. Taking the distribution map in 2016 (Fig. 3) as an example, it shows that BOWs are concentrated in Liwan District and Haizhu District. To present the BOWs distribution in these parts more clearly, Fig. 4 displays the partial views of BOW detection results, which illustrated a progressively declined tendency of BOW bodies. BOW bodies were mainly observed in narrow rivers in central urban areas, with the largest number in Liwan District.

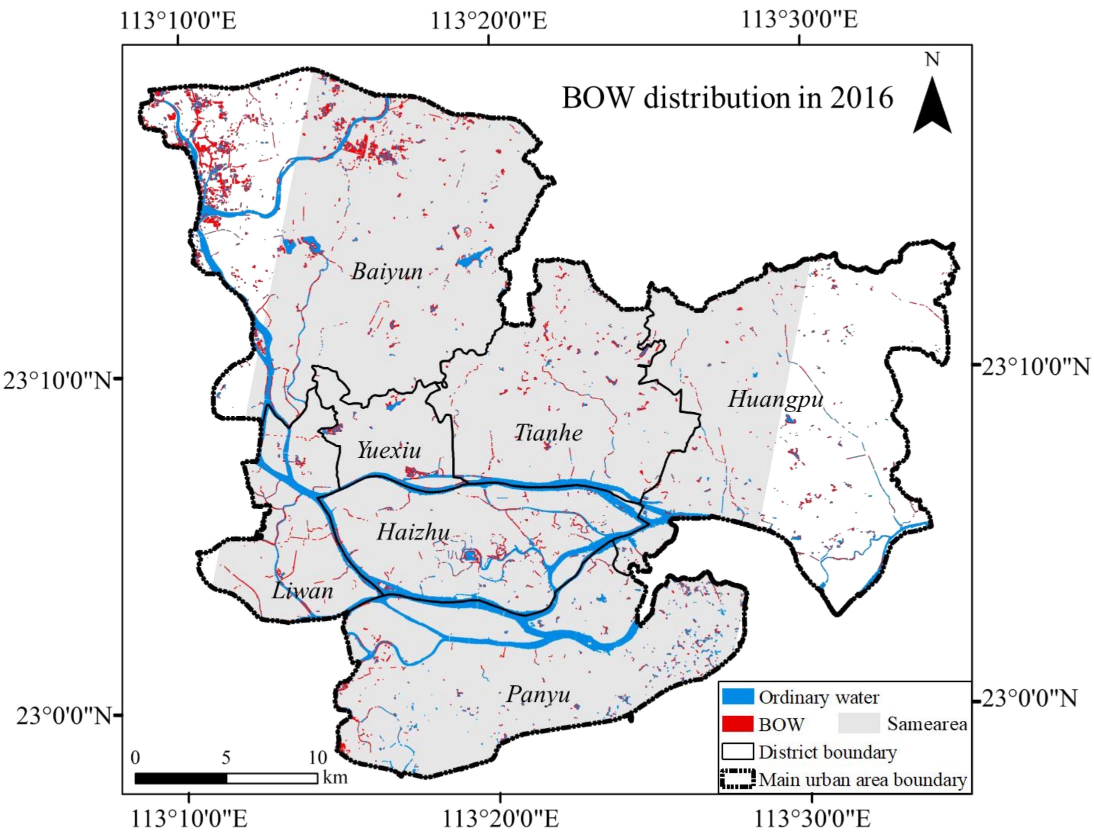

Fig. 3 Spatial distribution of BOW in 2016 of the study area

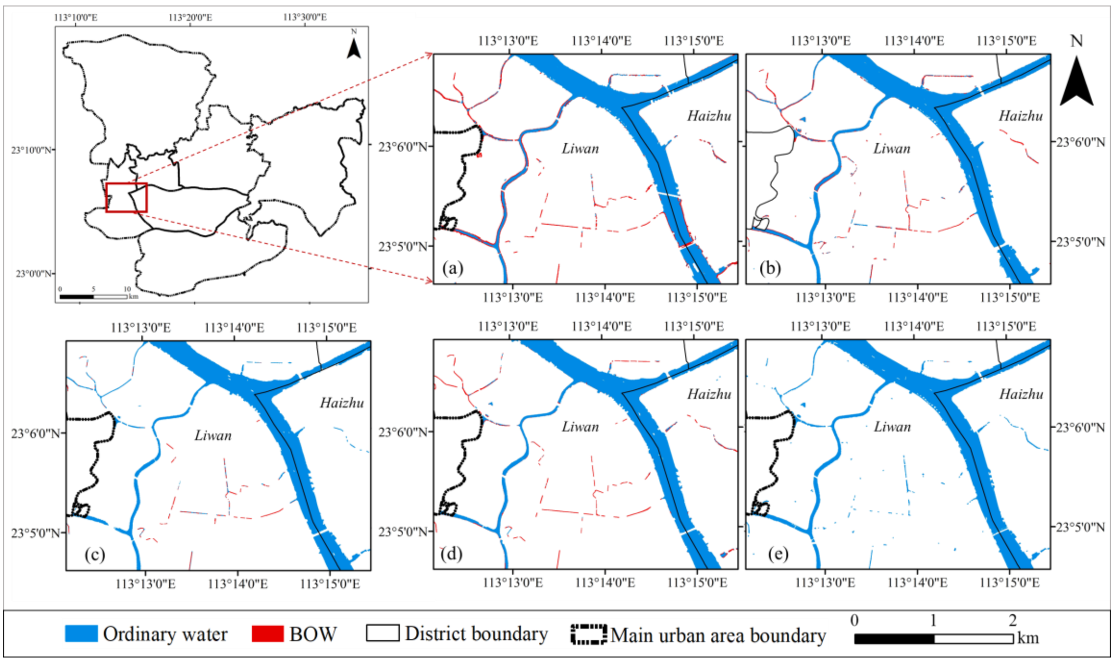

Fig. 4 Partial views for the spatial distribution of BOW bodies in 2016-2020, corresponding to (a)-(e) respectively. The spatial distribution of BOWs for an entire study area were shown in Fig. S4.

To quantitatively analyze BOW changes in various districts, the BOW distribution maps (Fig. S4) were statistically counted year by year (Table 4). Due to the availability of images, not all areas were covered every year, the calculation was performed in the overlap area of 5 years of images, labeled with ‘Samearea’ in Fig. 3. During the study period, a decreasing trend of BOW areas was observed in all districts. By 2020, no BOWs were observed in three districts, specifically, Yuexiu, Haizhu, and Panyu.

Table 4. Statistical results of the area of BOW and ORW identified in 2016-2020

Water type	**ORW (ha)**					**BOW (ha)**				
District	**2016**	**2017**	**2018**	**2019**	**2020**	**2016**	**2017**	**2018**	**2019**	**2020**
Yuexiu	204.71	201.14	175.28	190.42	195.27	28.55	12.58	0.35	7.04	0
Tianhe	348.81	337.53	337.42	310.02	361.77	34.59	38.30	3.57	18.85	1.18
Liwan	497.32	528.82	507.88	487.45	537.72	53.25	12.84	3.23	12.50	0.05
Huangpu	261.85	282.11	280.71	270.62	299.47	19.22	14.28	1.61	6.78	0.82
Haizhu	1009.06	942.00	1092.44	1088.94	1144.77	50.24	18.04	1.36	8.68	0
Panyu	1115.02	1014.31	1330.89	1281.97	1391.79	56.53	43.88	1.50	17.23	0
Baiyun	529.18	668.60	626.48	550.08	655.50	205.13	75.59	2.00	57.95	0.88
Total area	3965.95	3974.50	4351.11	4179.50	4586.28	447.52	215.51	13.62	129.03	2.93
Areal percentage	89.86%	94.86%	99.69%	97.01%	99.94%	10.14%	5.14%	0.31%	2.99%	0.06%

Quantitative zoning statistics were also conducted from the perspective of BOW management. Considering the water bodies extracted from GF images are greater than 2 m in width, excessively narrow rivers that cannot be identified in section 2.4.3 and rivers of discontinuous occurrence within 5 years were excluded. The total number of rivers and lakes counted here is 97, dispersedly distributed in 7 districts, namely, 3 in Yuexiu District, 13 in Tianhe District, 30 in Liwan District, 7 in Huangpu District, 13 in Haizhu District, 15 in Panyu District, and 16 in Baiyun District respectively. The study area includes 23 rivers listed as "35 BOW bodies in Guangzhou", 24 rivers in "50 BOW bodies", 46 rivers in "112 BOW bodies" (http://swj.gz.gov.cn/mssw/sjfb/content/post_6900098.html), and 4 important water bodies. The basic principle of zonal statistics is that as long as the length of BOW in a continuous river reaches 1/3, the river segment is judged as a BOW body, which overcomes the limitation of determining BOW levels by a sampling point.

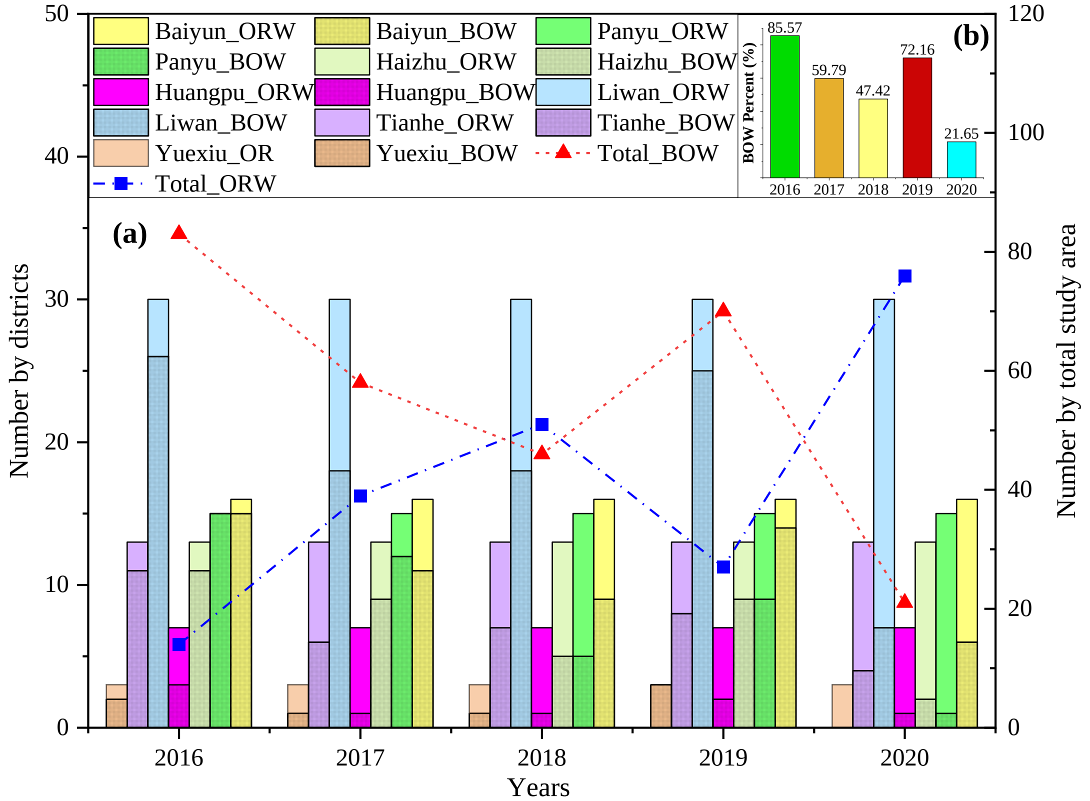

Fig. 5 Zonal statistics for multi-year BOW detection results. (a) shows the number of BOW and ORW changes by various districts and the total number by the whole study area. (b) exhibits the percentage of volume for BOW bodies over the years. The detailed amount of detected BOW bodies for each district were shown in Table S3 and Table S4.

Across the whole study area, the number of BOW bodies shows a general decreasing trend from 2016 to 2020, and it dropped to about 1/4 of what it was in 2016(85.57%) by 2020(21.65%). Correspondingly, there is a yearly increase in the number of ORW. The results indicate that BOW bodies have been progressively treated, but they have not been eliminated. These trends in BOW quantities indicate poor water quality in 2016-2017 and a significant improvement from 2017 onward. However, there is a rebound (72.16%) of BOW bodies in 2019 and the highest number of BOW bodies remained in Liwan District. In 2016-2017, BOW bodies were mainly distributed in Liwan District, Baiyun District, Panyu District, and Tianhe District; and then, BOW bodies were largely detected in Liwan District, Baiyun District, and Tianhe District in 2018-2020. There were relatively fewer BOW bodies in Huangpu and Yuexiu districts, showing their better river water quality.

3.3. The effects of climate change on BOWs

Correlation analysis (Fig. 6) and contribution calculations of BOW factors (Fig. 7) were performed to quantify the relationship between environmental factors and BOW and the factors' effects on BOW. Firstly, there was a strong positive correlation between BIR and BOW-area (r=0.60, p<0.05), which confirmed the rationality of the BIR model from another perspective. However, precipitation(r=-0.085) and temperature(r=-0.057) showed weak and negative correlations with BOW-area. Therefore, an increase in temperature and precipitation will cause the intensification of BOW. Meanwhile, there was a strong correlation between Pre and Tmp (r=0.74).

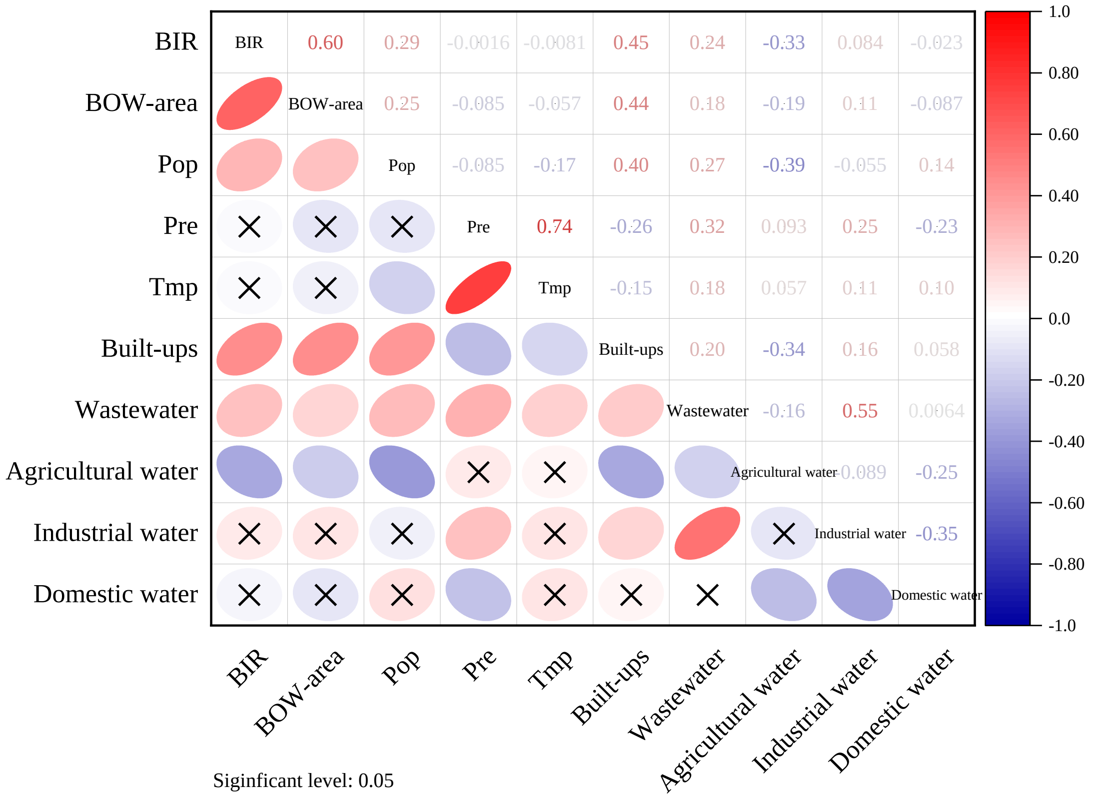

Fig. 6 Correlation coefficients between BOW and environmental factors. The X sign represents the insignificant correlation at the significance level of 0.05.

For the entire study area, temperature contributed 4.4% while precipitation only contributed 0.2% to the BOW (Fig. 7). However, the impacts of climate change on BOW varied greatly across different sub-regions. Precipitation contributed more to the BOW in the HaP district (5.2%) than in other areas and its contribution to BOW was higher than that of temperature in the HaP, L, and B districts. This suggests that precipitation has a greater impact on BOW in the HaP district than in other areas, and that its effect is larger than that of temperature. In the YTH sub-region, the contribution of temperature (17.9%) was higher than in other areas. Only in the YTH did the combined contribution of natural factors exceed that of human activities, indicating that the BOW in this area was more significantly affected by climate change. Therefore, the slightly increasing temperature and precipitation over years increase the risk of BOW occurrence, particularly in YTH.

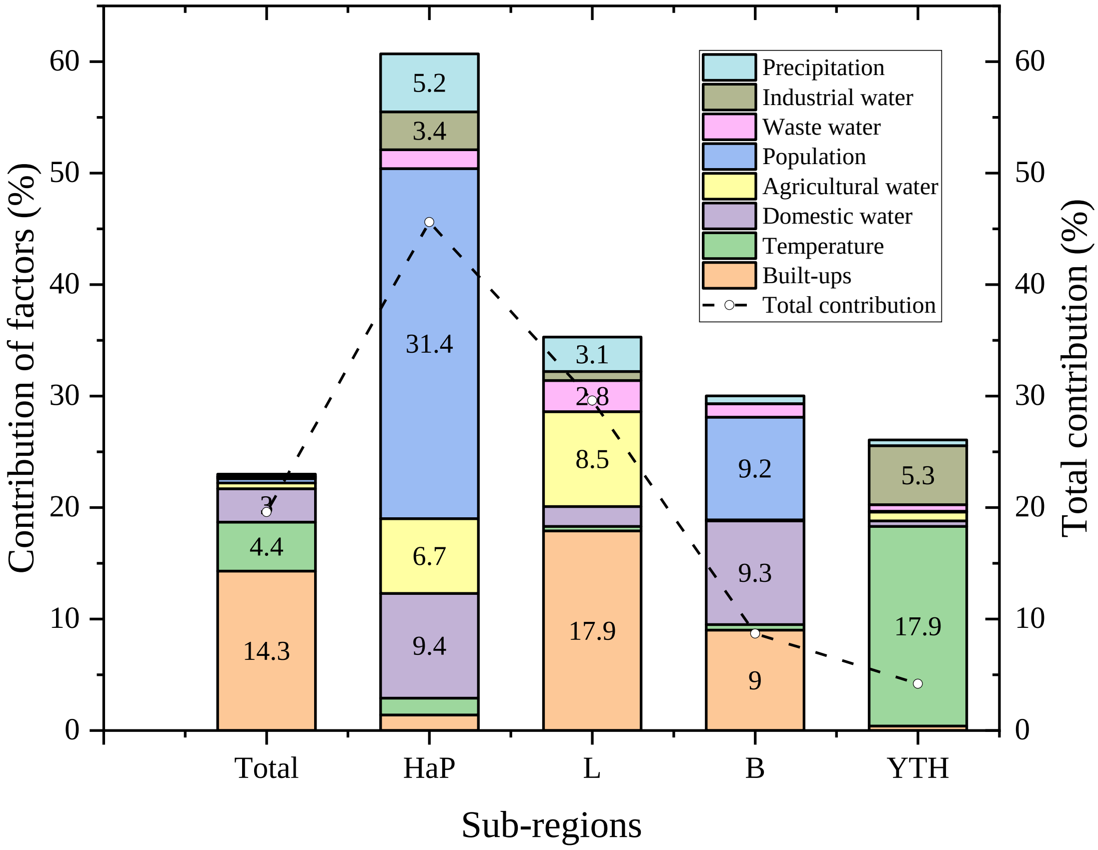

Fig. 7 The relative and total contribution rates of the environmental factors in the BOW-area. And the total contribution rates represent the adjusted explained variation of explanatory variables in RDA. The total contribution of all factors was lower than the sum of all factors for the covariance between environmental factors. The detailed contribution rates of factors were shown in Table S5.

Notably, natural factors may not have a consistent correlation with and contribution to BOW in different districts. For example, although the correlation between temperature and BOW is lower than that(r=0.18) between Wastewater and BOW in the entire area, the contribution of temperature to BOW is higher than that of Wastewater (0.1%). This is because the correlation coefficient measures only the linear relationship between environmental factors and BOW, while the RDA model further explores the nonlinear relationship and takes into account the influence of other factors. The high correlation(r=0.55) between wastewater and industrial water use reduces its explanatory power for BOW after accounting for the effect of industrial water use. Therefore, this further underscores the necessity of dividing the study area into different sub-regions for separate analysis, and not overlooking the impact of temperature and precipitation on BOW by solely relying on correlation analysis.

3.4. Contributions of anthropogenic drivers to BOWs

The correlation analysis (Fig. 6) revealed that anthropogenic factors had a stronger correlation with BOW-area than natural factors. BOW-area had a significantly positive correlation with Pop, Built-ups, and Wastewater, while there was a significant negative correlation with Agricultural water. Built-ups exhibited the highest relationship among the anthropogenic drivers, with a correlation coefficient of 0.44 and a p-value of <0.05, followed by Pop and Wastewater.

There are significant variations in the impact of human activities on BOW occurrence in the entire study area and its sub-regions. In the entire study area, the largest contributors to BOW were Build-ups with 14.3% and followed by Tmp and Domestic water (as shown in Fig. 7). Similar to natural factors, BOW in the sub-regions was affected to varying degrees by anthropogenic factors. In the HaP sub-region, Pop contributed the most with 31.4%, followed by Domestic water and Agricultural water. Built-ups accounted for the largest contribution in L with 17.9%, followed by Agricultural water. Pop and Domestic water were the main contributors to BOW in both HP and B districts. In the YTH sub-region, climate change, namely the Tmp here, had the largest effect on BOW, and Industrial water had a higher contribution compared to other districts. Overall, human activities had a greater impact on BOW occurrence than climate change in the main urban area of Guangzhou.

4. Discussion

4.1. Applicability of the BIR model

The BIR model using high spatial resolution remote sensing images enables fast and accurate identification of the spatial-temporal variations in BOW, which lays the foundation for studying the relationship between climate change adaptation and BOWs. Image reflectance of BOW in B, G, and R bands is lower than that of ordinary water (Fig. S1(b)), due to the low reflectance of dark and suspended particles in BOW bodies(Duan et al., 2014). Therefore, the BIR model takes advantage of the differences in central wavelength between NIR and R, and G and R, achieving good BOW identification, and should be applicable to other images of similar band design to Gaofen.

Additionally, ASTB facilitated the model application to different ground conditions and high-resolution remotely sensed images.

Furthermore, the BIR model would be applicable to identify BOWs in typical southern urban rivers that are of relatively high TSS concentrations. In a typical northern city like Taiyuan, the image reflectance of ordinary water bodies in the Red band is higher than that in the Green band(Li et al., 2019a). In contrast, in the southern rivers, the high TSS levels result in higher image reflectance in the Green band (Xu et al., 2021a). Ordinary water rich in suspended sediment is therefore likely to be mistakenly recognized as BOW by existing models, particularly for tidal rivers in estuarine zones in southern China(Shen et al., 2019). Compared to previously published BOW models built for northern urban rivers with accuracies of more than 80%(Li et al., 2019a; Qi et al., 2020; Shen et al., 2019), the BIR model exhibits better performance.

4.2. BOW variations in the context of climate change adaptation

From 2016 to 2020, BOW showed a downward trend overall (Fig. 5) benefiting from the vigorous promotion of policies in water management under climate change adaptation. DO was relatively low in general, while NH_3N showed a decreasing trend year by year (Fig. S3(b)(d)). The high correlation ($r=0.94$, $p<0.05$) between NH_3N and TP (Fig. S5) indicates that the area is significantly influenced by human activities. High concentrations of NH_3N in 2016 could be linked to increased nutrient delivery to urban rivers from industrial facilities, wastewater treatment factories(Song et al., 2021; Zhu et al., 2022), and sewage discharges (Fang et al., 2022). Since 2016, Guangzhou has implemented a series of climate change adaptation measures (as described in section 2.1) which have weakened BOW drivers, and in turn mitigated BOW occurrence. Since 2017, the key factor of BOW was transformed to DO. Although the number of BOW bodies identified in 2019 suddenly increased for the excess of DO, NH_3N was only partially exceeded (Fig. S3). Accordingly, the water quality has improved greatly, compared to the previous situations(Cao et al., 2020).

The dominant driving factors of BOW bodies have shown obvious regional characteristics. The largest number of BOW bodies occurred in the Liwan District, which depicted the negative impacts from the factors with relatively higher contributions(Built-ups and Agricultural water), associated with faster economic development and higher wastewater discharge(Bhat et al., 2021). Flower industries in Guangzhou are mainly concentrated in Liwan District, so Agricultural water and

Wastewater had an important impact on rivers. The dense distribution of urban areas and the long absence of dredging in some rivers increased the risks of BOW bodies and the difficulty of pollution tackling(Rong et al., 2020). In the HaP sub-region, Pop and Domestic water performed better in explaining BOW variations, indicating that domestic wastewater discharge was the dominant factor. Haizhu and Panyu districts have cleaned up and rectified many "scattered and disorganized" sites after the implementation of the river chief system, including the closure of small printing and dyeing workshops, cracking down on illegal acts of discharging polluted water, and increasing investment for the construction of sewage networks, which reduced the amount of industrial water use and wastewater discharge (Fig. S6). There were relatively fewer BOW bodies in the YTH and a clear declining trend, with BOW almost no longer emerging until 2020. Tmp and Industrial water were core factors that dominated the BOW-area in these districts, resulting from the weaker impact of Built-ups in urban areas with relatively high vegetation coverage. In addition, COVID-19 has brought a halt to production in some factories(Braga et al., 2022), and therefore, a decrease in industrial wastewater discharge(Yunus et al., 2020) in 2020(Fig. S6), and a possible increase in domestic wastewater emission, which may influence the BOW variation.

Furthermore, the overall contribution was lower than the explanatory degree of each factor(Fig. 7) because of the correlations between these factors(Chen et al., 2018). The total contribution of the 8 factors ranged from 4.2% to 45.6%, suggesting the possibility of other unconsidered factors(Du et al., 2022b; Fang et al., 2022) that were not considered in controlling the interannual changes in BOW for the data unavailability, and other potential factors such as the wastewater treatment investment. The instability of driving factors may be caused by limited 5 years of BOW variations. Accordingly, future studies on BOW changes should focus on combining long-term, high-resolution satellite images and water quality monitoring data to identify potential factors.

4.3. Uncertainty and limitations

The BIR model adopted a single parameter method to determine the BOW level, which may cause errors and occasionally even differences (Lyu et al., 2022). Firstly, water quality changes reveal that BOW bodies are mainly attributed to the combined effect of DO and NH_3N. Except for 2016, SD was higher than 25 cm (Fig. S3(a)). TP in most BOW bodies was higher than 0.4 mg/L (Fig. S3(c)), while the standard value(40mg/L) of COD (Fig. S3(e)) is not exceeded. Besides, BIR showed a positive correlation ($r=0.40$, $p<0.05$) with NH_3N, and a negative correlation with DO and SD (Fig. S5). This further proves that the controlling indicators of BOW in Guangzhou were NH_3N and DO.

What's more, the optimal thresholds of the BIR model and OA of BOW recognitions were calculated by three different standards, namely, NH_3N, DO, and $NH_3N \cup DO \cup SD$ (Table 5), to compare the difference between the three methods for identification results. The highest OA was based on the determination of any one of the three indicators, followed by a single NH_3N method and the lowest accuracy for a single DO standard. The result justifies the use of the single indicator determination method adopted in section 2.3.

Table 5. BIR model thresholds and BOW recognition accuracy under different discriminant criteria

Standards	**NH_3N**		**DO**		**$NH_3N \cup DO \cup SD$**	
Year	Optimal threshold	OA	Optimal threshold	OA	Optimal threshold	OA
2016	0.258	83.3%	1.964	66.7%	0.258	91.7%
2017	0.760	82.2%	-1.639	56.3%	0.544	87.5%
2018	2.941	95.0%	3.020	90.0%	2.941	90.0%
2019	3.757	83.3%	8.910	70.0%	2.081	90.0%
2020	0.622	88.7%	0.622	90.3%	0.622	90.3%

In addition, there are some other limitations that should be addressed, such as the limited number of GF images and seasonal water quality data(Lyu et al., 2022; Nukapothula et al., 2019). Therefore, increasing the amount and spatial density of automatic water quality monitoring stations can improve the accuracy of the rapid identification of BOW bodies. Besides, the availability of month-scale data corresponding to climate change adaptation measures (such as the amount of domestic wastewater discharged and investment in wastewater treatment) would better assess the impact of climate change adaptation on BOW.

Additionally, due to data unavailability and the complexity of factors influencing BOW, the present study reveals the annual spatial distribution of BOWs in the context of climate change adaption. Causes of BOW are very complex and are easily influenced by stochastic human activities. For example, one of the direct driving factors of BOW is the amount of wastewater discharge, which is related to the optimization of urban pipe networks and sewage treatment facilities and may even be affected by other non-climate change adaptation measures. Further exploration is needed to elucidate the direct contribution of climate change adaptation measures to BOWs and its mechanism.

4.4. Implications for management and policymaking

Quantitative identification of BOW from time-series satellite images enables rapid monitoring of water pollution and scientific assessment for the effectiveness of BOW treatment. Spatial-temporal variations of BOW bodies in Guangzhou have shown that there was a significant improvement in water quality during 2016-2020, as a result of active implementation of water pollution control and climate change adaptation measures. However, strong risks of potential re-blackening exist in BOW bodies, such as the sudden increase in BOW occurrence in 2019. The identification of BOW bodies can help to quickly locate the key river sections to be treated. For example, Liwan District and Baiyun District still maintained a higher number of BOW bodies than other regions in 2020, despite some modest decreases in Wastewater discharge which have been recorded beginning in 2019 (Fig. S6). The BOW changes also enable the manager to grasp whether the policy is being implemented in the region and whether water treatment under climate change adaptation is making a difference to the improvement of the BOW phenomenon.

Furthermore, studying the drivers of BOW will assist in the development of accurate policies and effective climate change adaptation measures for managing those environmental factors in local districts, to adapt to and mitigate the impacts of climate change and human activities on urban water environment to reduce BOW bodies. In the study area, the variations of BOW bodies were mainly correlated with Built-ups, Tmp, and Domestic water. Corresponding climate change measures need to be implemented with a priority. On the one hand, the impact of urbanization on water quality would be mitigated to some extent by rational planning of urban layout and functions, such as increasing green space coverage and urban park areas, and enhancing the effectiveness of ecosystems in purifying water quality. On another hand, increased investment in domestic wastewater treatment and strict control of discharges can promote the reduction of BOW bodies. Meanwhile, the dominant factors of BOW changes vary in different regions, suggesting that tailored management for controlling drivers would be more effective for treating BOWs. Taking the Liwan district as an example, increasing urban greenery and improving water-saving irrigation should be prioritized.

5. Conclusions

With a BOW model constructed for identification BOWs in urban areas using high spatial resolution Gaofen images, the annual dynamics of BOW distribution from 2016 to 2020 in Guangzhou was explored in the context of climate change adaption. The main findings are summarized as follows:

(1) The number of BOW bodies in the main urban area of Guangzhou showed a decreased tendency from 83 in 2016 to 21 in 2020, despite a re-blackening situation in 2019, illustrating that direct pollution control in the context of climate change adaptation measures has promoted water quality in the urban rivers.

(2) BOW changes in different regions are dominated by distinct drivers. Human activities exhibited a more important role in the annual variations of BOW bodies. Appropriate climate change measures are required to fine-tune the management of BOW by mitigating those anthropogenic drivers and improving the efficiency and effectiveness of water quality optimization.

(3) The BOW detection method aided by an automatic threshold selection algorithm has prompted the expeditious identification of BOWs fed with Gaofen images. This method facilitates quick monitoring of spatial-temporal dynamics of small BOWs in urban area with images of similar band design to Gaofen, and generates basic data required for exploring the direct contribution of climate change adaptation measures to BOWs and its mechanism.

Acknowledgment

Acknowledgment for the data supports from "Loess Plateau SubCenter, National Earth System Science Data Sharing Infrastructure, National Science & Technology Infrastructure of China (http://loess.geodata.cn)", and "Guangdong Center of Data and Application with High Resolution Earth Observation System (http://gdgf.gd.gov.cn/GDGF_Portal/index.jsp)".

Statements and Declarations

Author Contributions: All authors contributed to the study conception and design. **Tianhong Li*** designed the research and edited the manuscript; **Bing Liu** designed and performed the research, and prepared the draft; **Haojun Xi** contributed to the introduction and edited the manuscript. The first draft of the manuscript was written by **Bing Liu** and all authors commented on previous versions of the manuscript. **Alistair G.L. Borthwick** contributed to international background, consummated the methodology. All authors read and approved the final manuscript.

Competing Interests: The authors declare no competing interests.

References

Babaeian, F., Delavar, M., Morid, S., Srinivasan, R., 2021. Robust climate change adaptation pathways in agricultural water management. Agr Water Manage. 252.https://dx.doi.org/10.1016/j.agwat.2021.106904.

Barnes, B.B., Hu, C., Holekamp, K.L., Blonski, S., Spiering, B.A., et al., 2014. Use of Landsat data to track historical water quality changes in Florida Keys marine environments. Remote Sens Environ. 140, 485-496.https://doi.org/10.1016/j.rse.2013.09.020.

Bartlett, J.A., Dedekorkut-Howes, A., 2022. Adaptation strategies for climate change impacts on water quality: a systematic review of the literature. J Water Clim Change.https://dx.doi.org/10.2166/wcc.2022.279.

Berrang-Ford, L., Siders, A.R., Lesnikowski, A., Fischer, A.P., Callaghan, M.W., et al., 2021. A systematic global stocktake of evidence on human adaptation to climate change. Nat Clim Change. 11(11), 989-+.https://dx.doi.org/10.1038/s41558-021-01170-y.

Bhat, S.U., Khanday, S.A., Islam, S.T., Sabha, I., 2021. Understanding the spatiotemporal pollution dynamics of highly fragile montane watersheds of Kashmir Himalaya, India. Environ Pollut. 286, 117335.https://doi.org/10.1016/j.envpol.2021.117335.

Bie, W., Fei, T., Liu, X., Liu, H., Wu, G., 2020. Small water bodies mapped from Sentinel-2 MSI (MultiSpectral Imager) imagery with higher accuracy. Int J Remote Sens. 41(20), 7912-7930.https://doi.org/10.1080/01431161.2020.1766150.

Biswas, R.R., Sharma, R., Gyasi-Agyei, Y., 2022. Adaptation to climate change: A study on regional urban water management and planning practice. J Clean Prod. 355.https://dx.doi.org/10.1016/j.jclepro.2022.131643.

Braga, F., Ciani, D., Colella, S., Organelli, E., Pitarch, J., et al., 2022. COVID-19 lockdown effects on a coastal marine environment: Disentangling perception versus reality. Sci Total Environ. 817, 153002.https://doi.org/10.1016/j.scitotenv.2022.153002.

Cao, J., Sun, Q., Zhao, D., Xu, M., Shen, Q., et al., 2020. A critical review of the appearance of black-odorous waterbodies in China and treatment methods. J Hazard Mater. 385, 121511.https://doi.org/10.1016/j.jhazmat.2019.121511.

Cao, Z., Ma, R., Melack, J.M., Duan, H., Liu, M., et al., 2022. Landsat observations of chlorophyll-a variations in Lake Taihu from 1984 to 2019. Int J Appl Earth Obs. 106, 102642.https://doi.org/10.1016/j.jag.2021.102642.

Cardew, P.T., 2003. A method for assessing the effect of water quality changes on plumbosolvency using random daytime sampling. Water Res. 37(12), 2821-2832.https://doi.org/10.1016/S0043-1354(03)00120-9.

Chen, G., Luo, J., Zhang, C., Jiang, L., Tian, L., et al., 2018. Characteristics and influencing factors of spatial differentiation of urban black and odorous waters in China. Sustainability. 10(12), 4747.https://doi.org/10.3390/su10124747.

Chen, Z., Dou, M., Xia, R., Li, G., Shen, L., 2022. Spatiotemporal evolution of chlorophyll-a concentration from MODIS data inversion in the middle and lower reaches of the Hanjiang River, China. Environ Sci Pollut Res.https://doi.org/10.1007/s11356-021-18214-7.

Cheng, X., Chen, L., Sun, R., Kong, P., 2018. Land use changes and socio-economic development strongly deteriorate river ecosystem health in one of the largest basins in China. Sci Total Environ. 616-617, 376-385.https://doi.org/10.1016/j.scitotenv.2017.10.316.

Cherkauer, K.A., Bowling, L.C., Byun, K., Chaubey, I., Chin, N., et al., 2021. Climate change impacts and strategies for adaptation for water resource management in Indiana. Climatic Change. 165(1-2).https://dx.doi.org/10.1007/s10584-021-02979-4.

Development and Reform Commission of Guangdong Province, 2017. The 13th Five-Year Plan for Climate Change Programme in Guangdong Province(in Chinese). http://drc.gd.gov.cn/gkmlpt/content/1/1060/post_1060342.html#4146. (Accessed 10 May 2023).

Development and Reform Commission of Guangdong Province, 2022. The 14th Five-Year Plan for Climate Change Programme in Guangdong Province(in Chinese). http://gdee.gd.gov.cn/attachment/0/494/494368/3977041.pdf. (Accessed 17 March 2023).

Du, C., Li, Y., Lyu, H., Shi, K., Liu, N., et al., 2022a. Characteristics of the total suspended matter concentration in the Hongze Lake during 1984–2019 based on Landsat data. Remote Sens. 14(12), 2919.https://doi.org/10.3390/rs14122919.

Du, Y., Song, K., Wang, Q., Li, S., Wen, Z., et al., 2022b. Total suspended solids characterization and management implications for lakes in East China. Sci Total Environ. 806, 151374.https://doi.org/10.1016/j.scitotenv.2021.151374.

Duan, H., Ma, R., Loiselle, S.A., Shen, Q., Yin, H., et al., 2014. Optical characterization of black water blooms in eutrophic waters. Sci Total Environ. 482-483, 174-183.https://doi.org/10.1016/j.scitotenv.2014.02.113.

Estrada, F., Botzen, W.J.W., Tol, R.S.J., 2017. A global economic assessment of city policies to reduce climate change impacts. Nat Clim Change. 7(6), 403-+.https://dx.doi.org/10.1038/nclimate3301.

Fang, C., Song, K., Paerl, H.W., Jacinthe, P.A., Wen, Z., et al., 2022. Global divergent trends of algal blooms detected by satellite during 1982–2018. Global Change Biol. 28(7), 2327-2340.https://doi.org/10.1111/gcb.16077.

He, Y., Song, N., Jiang, H.-L., 2018. Effects of dissolved organic matter leaching from macrophyte litter on black water events in shallow lakes. Environ Sci Pollut Res. 25(10), 9928-9939.https://doi.org/10.1007/s11356-018-1267-0.

Hersbach, H., Bell, B., Berrisford, P., Hirahara, S., Horanyi, A., et al., 2020. The ERA5 global reanalysis. Q J Roy Meteor Soc. 146(730), 1999-2049.https://dx.doi.org/10.1002/qj.3803.

Hladyz, S., Watkins, S.C., Whitworth, K.L., Baldwin, D.S., 2011. Flows and hypoxic blackwater events in managed ephemeral river channels. J Hydrol. 401(1), 117-125.https://doi.org/10.1016/j.jhydrol.2011.02.014.

Hu, M., Ma, R., Xiong, J., Wang, M., Cao, Z., et al., 2022. Eutrophication state in the Eastern China based on Landsat 35-year observations. Remote Sens Environ. 277, 113057.https://doi.org/10.1016/j.rse.2022.113057.

Jones, E.R., Bierkens, M.F.P., Wanders, N., Sutanudjaja, E.H., Van Beek, L.P.H., et al., 2022. Current wastewater treatment targets are insufficient to protect surface water quality. Commun Earth Environ. 3(1).https://dx.doi.org/10.1038/s43247-022-00554-y.

Legendre, P., Legendre, L., 2012. Numerical ecology, Third English ed. Elsevier, Amsterdam.

Li, J., Li, J., Zhu, L., Shen, Q., Dai, H., et al., 2019a. Remote sensing identification and validation of urban black and odorous water in Taiyuan city (in Chinese). Nat Remote Sens Bull. 23(4), 773-784.https://doi.org/10.11834/jrs.20197292.

Li, S., Peng, S., Jin, B., Zhou, J., Li, Y., 2019b. Multi-scale relationship between land use/land cover types and water quality in different pollution source areas in Fuxian Lake Basin. PeerJ. 7, e7283.https://doi.org/10.7717/peerj.7283.

Li, W., Lin, S., Wang, W., Huang, Z., Zeng, H., et al., 2020a. Assessment of nutrient and heavy metal contamination in surface sediments of the Xiashan stream, eastern Guangdong Province, China. Environ Sci Pollut Res. 27(21), 25908-25924.https://doi.org/10.1007/s11356-019-06912-2.

Li, X., Gong, P., Zhou, Y., Wang, J., Bai, Y., et al., 2020b. Mapping global urban boundaries from the global artificial impervious area (GAIA) data. Environ Res Lett. 15(9), 094044.https://doi.org/10.1088/1748-9326/ab9be3.

Liao, Z.L., Zhi, G.Z., Zhou, Y.W., Xu, Z.X., Rink, K., 2016. To analyze the Urban Water Pollution Discharge System using the tracking and tracing approach. Environ Earth Sci. 75(14).https://dx.doi.org/10.1007/s12665-016-5881-1.

Lin, Y., Li, L., Yu, J., Hu, Y., Zhang, T., et al., 2021. An optimized machine learning approach to water pollution variation monitoring with time-series Landsat images. Int J Appl Earth Obs. 102, 102370.https://doi.org/10.1016/j.jag.2021.102370.

Liu, S., Fu, R., Liu, Y., Suo, C., 2022. Spatiotemporal variations of water quality and their driving forces in the Yangtze River Basin, China, from 2008 to 2020 based on multi-statistical analyses. Environ Sci Pollut Res. 29(46), 69388-69401.https://doi.org/10.1007/s11356-022-20667-3.

Liu, X., Zhang, Y., Li, Z., Li, P., Xu, G., et al., 2021. Response of water quality to land use in hydrologic response unit and riparian buffer along the Dan River, China. Environ Sci Pollut Res. 28(22), 28251-28262.https://doi.org/10.1007/s11356-021-12636-z.

Lyu, L., Song, K., Wen, Z., Liu, G., Shang, Y., et al., 2022. Estimation of the lake trophic state index (TSI) using hyperspectral remote sensing in Northeast China. Opt Express. 30(7), 10329-10345.https://doi.org/10.1364/OE.453404.

Malhi, Y., Franklin, J., Seddon, N., Solan, M., Turner, M.G., et al., 2020. Climate change and ecosystems: threats, opportunities and solutions. Philos T R Soc B. 375(1794).https://dx.doi.org/10.1098/rstb.2019.0104.

Miao, S., Lyu, H., Xu, J., Bi, S., Guo, H., et al., 2021. Characteristics of the chromophoric dissolved organic matter of urban black-odor rivers using fluorescence and UV–visible spectroscopy. Environ Pollut. 268, 115763.https://doi.org/10.1016/j.envpol.2020.115763.

Ministry of Housing and Urban-Rural Development of the People’s Republic of China, 2015. The Chinese Government’s Guideline for Urban Black and Odorous Water Treatment(in Chinese). http://www.mohurd.gov.cn/wjfb/201509/W020150911050936.pdf. (Accessed 17 March 2023).

Ministry of Housing and Urban-Rural Development of the People’s Republic of China, 2021. China will basically eliminate urban black and smelly water bodies by the 14th Five-Year Plan(in Chinese). http://www.mohurd.gov.cn/zxydt/202104/t20210406_249689.html. (Accessed 17 March 2023).

Norgbey, E., Li, Y., Zhu, Y., Nwankwegu, A.S., Bofah-Buah, R., et al., 2021. Combined use of high-resolution dialysis, diffusive gradient in thin films (DGT) technique, and conventional methods to assess trace metals in reservoir sediments. Environ Monit Assess. 193(8), 469.https://doi.org/10.1007/s10661-021-09247-z.

Nukapothula, S., Chen, C., Wu, J., 2019. Long-term distribution patterns of remotely sensed water quality variables in Pearl River Delta, China. Estuarine, Coastal Shelf Sci. 221, 90-103.https://doi.org/10.1016/j.ecss.2019.02.038.

People's Government of Guangdong Province, 2011. Responding to climate change in Guangdong Province(in Chinese). https://www.gd.gov.cn/gkmlpt/content/0/139/post_139497.html#7 (Accessed 17 March 2023).

Qi, K., Shen, Q., Luo, X., Li, J., Yao, Y., et al., 2020. Remote sensing classification and recognition of black and odorous water in Shenyang based on GF-2 image (in Chinese). Remote Sens Technol Appl. 35(2), 424-434.https://doi.org/10.11873/j.issn.1004-0323.2020.2.0424.

Ren, J., Liang, J., Ren, B., Zheng, X., Guo, C., 2018. New patterns of temporal and spatial variation in water quality of a highly artificialized urban river-course—a case study in the Tongzhou section of the Beiyun River. Water. 10(10), 1446.https://doi.org/10.3390/w10101446.

Rixen, T., Baum, A., Sepryani, H., Pohlmann, T., Jose, C., et al., 2010. Dissolved oxygen and its response to eutrophication in a tropical black water river. J Environ Manage. 91(8), 1730-1737.https://doi.org/10.1016/j.jenvman.2010.03.009.

Robiou du Pont, Y., Jeffery, M.L., Guetschow, J., Rogelj, J., Christoff, P., et al., 2017. Equitable mitigation to achieve the Paris Agreement goals. Nat Clim Change. 7(1), 1-+.https://dx.doi.org/10.1038/nclimate3186.

Rong, N., Lu, W., Zhang, C., Wang, Y., Zhu, J., et al., 2020. In situ high-resolution measurement of phosphorus, iron and sulfur by diffusive gradients in thin films in sediments of black-odorous rivers in the Pearl River Delta region, South China. Environ Res. 189, 109918.https://doi.org/10.1016/j.envres.2020.109918.

Santy, S., Mujumdar, P., Bala, G., 2020. Potential Impacts of Climate and Land Use Change on the Water Quality of Ganga River around the Industrialized Kanpur Region. Sci Rep-Uk. 10(1).https://doi.org/10.1038/s41598-020-66171-x.

Sarigai, Yang, J., Zhou, A., Han, L., Li, Y., et al., 2020. Monitoring urban black-odorous water by using hyperspectral data and machine learning. Environ Pollut. 269, 116166.https://doi.org/10.1016/j.envpol.2020.116166.

Shen, Q., Yao, Y., Li, J., Zhang, F., Wang, S., et al., 2019. A CIE Color Purity Algorithm to Detect Black and Odorous Water in Urban Rivers Using High-Resolution Multispectral Remote Sensing Images. IEEE T GeoSci Remote. 57(9), 6577-6590.https://doi.org/10.1109/tgrs.2019.2907283.

Somasundaram, D., Zhang, F., Ediriweera, S., Wang, S., Yin, Z., et al., 2021. Patterns, trends and drivers of water transparency in Sri Lanka using Landsat 8 observations and Google Earth Engine. Remote Sens. 13(11), 2193.https://doi.org/10.3390/rs13112193.

Sonali, P., Kumar, D.N., 2020. Review of recent advances in climate change detection and attribution studies: a large-scale hydroclimatological perspective. J Water Clim Change. 11(1), 1-29.https://dx.doi.org/10.2166/wcc.2020.091.

Song, K., Fang, C., Jacinthe, P.-A., Wen, Z., Liu, G., et al., 2021. Climatic versus Anthropogenic Controls of Decadal Trends (1983–2017) in Algal Blooms in Lakes and Reservoirs across China. Environ Sci Technol. 55(5), 2929-2938.https://doi.org/10.1021/acs.est.0c06480.

Song, K., Wang, Q., Liu, G., Jacinthe, P.-A., Li, S., et al., 2022. A unified model for high resolution mapping of global lake (>1 ha) clarity using Landsat imagery data. Sci Total Environ. 810, 151188.https://doi.org/10.1016/j.scitotenv.2021.151188.

Song, Y., Song, X., Shao, G., Hu, T., 2020. Effects of land use on stream water quality in the rapidly urbanized areas: A multiscale analysis. Water. 12(4), 1123.https://doi.org/10.3390/w12041123.

Wai, K.M., Wang, X.M., Lin, T.H., Wong, M.S., Zeng, S.K., et al., 2017. Observational evidence of a long-term increase in precipitation due to urbanization effects and its implications for sustainable urban living. Science of The Total Environment. 599-600, 647-654.https://doi.org/10.1016/j.scitotenv.2017.05.014.

Wang, R., Xu, S., Jiang, C., Zhang, Y., Bai, N., et al., 2019a. Impacts of human activities on the composition and abundance of sulfate-reducing and sulfur-oxidizing microorganisms in polluted river sediments. Front Microbiol. 10.https://doi.org/10.3389/fmicb.2019.00231.

Wang, X., Deng, Y., Tuo, Y., Cao, R., Zhou, Z., et al., 2021. Study on the temporal and spatial distribution of chlorophyll a in Erhai Lake based on multispectral data from environmental satellites. Ecol Inform. 61, 101201.https://doi.org/10.1016/j.ecoinf.2020.101201.

Wang, Y., Shen, J., Yan, W., Chen, C., 2019b. Effects of Landscape Development Intensity on River Water Quality in Urbanized Areas. Sustainability. 11(24), 7120.https://doi.org/10.3390/su11247120.

Wang, Y., Yao, J., Yang, P., Zhang, Y., Sun, Y., et al., 2022. Dynamic remote sensing monitoring and its influence factors analysis for urban black and odorous water body management and treatment in Beijing, China (in Chinese). Chin J Environ Eng. 19(9), 3092-3101.https://doi.org/10.12030/j.cjee.202206034.

Wen, S., Wang, Q., Li, Y., Zhu, L., Lv, H., et al., 2018. Remote sensing identification of urban black-odor water bodies based on high-resolution images: A case study in Nanjing (in Chinese). Chin J Environ Sci. 39(1), 57-67.https://doi.org/10.13227/j.hjkx.201703264.

Xu, H., Xu, G., Wen, X., Hu, X., Wang, Y., 2021a. Lockdown effects on total suspended solids concentrations in the Lower Min River (China) during COVID-19 using time-series remote sensing images. Int J Appl Earth Obs. 98, 102301.https://doi.org/10.1016/j.jag.2021.102301.

Xu, J., Xu, Z.X., 2022. China sewage treatment engineering issues assessment. J Clean Prod. 377.https://dx.doi.org/10.1016/j.jclepro.2022.134391.

Xu, Z., Xu, J., Yin, H., Jin, W., Li, H., et al., 2019a. Urban river pollution control in developing countries. Nature Sustainability. 2(3), 158-160.https://dx.doi.org/10.1038/s41893-019-0249-7.

Xu, Z., Zhu, Z., Liu, S., Song, L., Wang, X., et al., 2021b. Evapotranspiration partitioning for multiple ecosystems within a dryland watershed: Seasonal variations and controlling factors. J Hydrol. 598, 126483.https://doi.org/10.1016/j.jhydrol.2021.126483.

Xu, Z.X., Qu, Y., Wang, S.Y., Chu, W.H., 2021c. Diagnosis of pipe illicit connections and damaged points in urban stormwater system using an inversed optimization model. J Clean Prod. 292.https://dx.doi.org/10.1016/j.jclepro.2021.126011.

Xu, Z.X., Xu, J., Yin, H.L., Jin, W., Li, H.Z., et al., 2019b. Urban river pollution control in developing countries. Nat Sustain. 2(3), 158-160.https://dx.doi.org/10.1038/s41893-019-0249-7.

Yi, X., Zhang, C., Liu, H., Wu, R., Tian, D., et al., 2019. Occurrence and distribution of neonicotinoid insecticides in surface water and sediment of the Guangzhou section of the Pearl River, South China. Environ Pollut. 251, 892-900.https://doi.org/10.1016/j.envpol.2019.05.062.

Yu, Z., Huang, Q., Peng, X., Liu, H., Ai, Q., et al., 2022. Comparative Study on Recognition Models of Black-Odorous Water in Hangzhou Based on GF-2 Satellite Data. Sensors. 22(12), 4593.https://doi.org/10.3390/s22124593.

Yunus, A.P., Masago, Y., Hijioka, Y., 2020. COVID-19 and surface water quality: Improved lake water quality during the lockdown. Sci Total Environ. 731, 139012.https://doi.org/10.1016/j.scitotenv.2020.139012.

Zhao, C., Zhang, Y., Guo, W., Fahad Baqa, M., 2022. Dynamics and drivers of water clarity derived from Landsat and in-situ measurement data in Hulun Lake from 2010 to 2020. Water. 14(8), 1189.https://doi.org/10.3390/w14081189.

Zhao, J., Lin, L., Yang, K., Liu, Q., Qian, G., 2015. Influences of land use on water quality in a reticular river network area: A case study in Shanghai, China. Landscape Urban Plan. 137, 20-29.https://doi.org/10.1016/j.landurbplan.2014.12.010.

Zhao, Y., Wang, S., Zhang, F., Shen, Q., Li, J., 2021. Retrieval and spatio-temporal variations analysis of Yangtze River water clarity from 2017 to 2020 based on Sentinel-2 images. Remote Sens. 13(12), 2260.https://doi.org/10.3390/rs13122260.

Zhou, X., Huang, Z., Wan, Y., Ni, B., Zhang, Y., et al., 2022. A new method for continuous monitoring of black and odorous water body using evaluation parameters: a case study in Baoding. Remote Sens. 14(2).https://doi.org/10.3390/rs14020374.

Zhu, B., Bai, Y., Zhang, Z., He, X., Wang, Z., et al., 2022. Satellite remote sensing of water quality variation in a Semi-Enclosed bay (Yueqing Bay) under strong anthropogenic impact. Remote Sens. 14(3), 550.https://doi.org/10.3390/rs14030550.